International Journal of Mechanical, Industrial and Aerospace Sciences
ISSN: 2517-9950
Vol:5, No:6, 2011

The Effects of Plate-Support Condition on Buckling Strength of Rectangular Perforated Plates under Linearly Varying In-Plane Normal Load

M. Tajdari, A. R. Nezamabadi, M. Naeemi and P. Pirali

***Abstract*—**Mechanical buckling analysis of rectangular plates with central circular cutout is performed in this paper. The finite-element method is used to study the effects of plate-support conditions, aspect ratio, and hole size on the mechanical buckling strength of the perforated plates subjected to linearly varying loading. Results show that increasing the hole size does not necessarily reduce the mechanical buckling strength of the perforated plates. It is also concluded that the clamped boundary condition increases the mechanical buckling strength of the perforated plates more than the simply-supported boundary condition and the free boundary conditions enhance the mechanical buckling strength of the perforated plates more effectively than the fixed boundary conditions. Furthermore, for the bending cases, the critical buckling load of perforated plates with free edges is less than perforated plates with fixed edges.

***Keywords*—**Buckling, Perforated plates, Boundary condition, Rectangular plates

I. Introduction

THIN plate elements are one of the main components in many structures such as ship hulls, dock gates, plate and box girders of bridges, platforms of offshore structures and aerospace structures. Cutout holes in such plate elements are necessary for inspection, maintenance, service purposes and weight reduction.

The presence of cutouts (perforations) in a structural member often complicates the design process. In aerospace structures, cutouts are commonly used as access ports for mechanical and electrical systems or specially weight reduction. Structural panels with cutouts often experience compressive loads that are induced either mechanically or thermally and can result in panel buckling. Thus, the buckling behavior of structural panels with cutouts must be fully assigned in designing process.

M. Tajdari is with the Islamic Azad University, Science and Research Branch, Department of Mechanical Engineering, Arak, Iran (phone: +988614134182-95; fax+988614134181; e-mail: tajdari@yahoo.com).

A. R. Nezamabadi is with the Islamic Azad University, Science and Research Branch, Department of Mechanical Engineering, Arak, Iran (e-mail: alireza.nezamabadi@gmail.com).

M. Naeemi is with the Mechanical Engineering Department, Ferdowsi University of Mashhad, Mashhad, Iran, (e-mail: nehezk_64@yahoo.com).

P. Pirali is with the Islamic Azad University, Science and Research Branch, Department of Mechanical Engineering, Arak, Iran (e-mail: ppirali@yahoo.com).

The buckling of flat square plates with central circular holes under in-plane edge compression has been studied both theoretically and experimentally by various authors [1–12]. The methods of theoretical analysis used by most of the past investigators [1–3, 5] were the Rayleigh-Ritz minimum energy method and the Timoshenko method [13]. However, except for Schlack [3] and Kawai and Ohtsubo [5], the theoretical analysis methods used do not allow the boundary and loading conditions to be precisely defined for larger hole sizes. Because the stress distribution of the infinite perforated plate are used as the prebuckling stress solution for the finite perforated plate. Thus, most of the earlier buckling solutions are limited to small hole sizes and are not fit for studying the effects of different plate boundary conditions on the buckling strengths of the finite plates with arbitrarily sized holes using these approximate solutions.

Schlack [3] analyzed the buckling behavior of a simply supported square plate with a circular hole, subjected to uniform edge displacements with three arbitrary displacement functions Using the Rayleigh-Ritz method and calculated the buckling displacements. Then, the buckling loads were calculated using stress-strain relationships. Ritchie and Rhodes [7] studied the buckling behavior of both square and rectangular simply-supported perforated plates. Their theoretical analysis employed an approximate approach using a combination of Rayleigh-Ritz and finite-element method. These methods are reasonably accurate for small holes, but lose accuracy when dealing with larger holes. The results of their analysis show that the buckling behavior of perforated rectangular plates is quite different from perforated square plates and the buckling mode is dependent on the hole size. Kawai and Ohtsubo [5] also studied the perforated square plates using the Rayleigh-Ritz procedure with the prebuckling stress distribution determined by the finite-element method. To reduce the labor of numerical calculations, the double integrations in the energy procedure for each finite element were transformed into line integrals around the element boundary using the well-known Gauss theorem. To minimize the mathematical complexities, Nemeth [8–11] analyzed perforated square orthotropic plates by converting the classical two-dimensional buckling analysis into an equivalent one dimensional analysis by approximating the plate displacements with kinematically admissible series. In his

analysis, the two unloaded edges were assumed simply supported, and the loaded edges were either simply supported or clamped. This approximate buckling analysis predicted the buckling loads to within 10 percent of those calculated using the finite-element method. Nemeth's analytical and experimental results [10] indicated that increasing the hole size in a given plate does not always reduce the 3 buckling load. Lee et al. [12] examined the buckling behavior of a square plate with a central circular hole using the finite-element method. This study was limited to small size holes.

Recent thin shell finite element research on the elastic buckling of simply-supported rectangular plates with multiple holes has demonstrated that the presence of holes can either decrease or increase the critical elastic buckling stress and change the length and quantity of buckled half-waves [15–19]. The elastic buckling behavior depends upon the quantity of hole material removed relative to the size of the plate and hole spacing. These recent findings are important as a design perspective. Because they demonstrate that certain hole location and geometry has very deleterious effect on critical elastic buckling stress and potentially load-deformation response. The most of past analyses of perforated plates considered mainly the plates under simply-supported boundary condition. In this paper we investigate the mechanical buckling analysis of rectangular plates containing arbitrarily-sized central circular holes. A finite-element method was used to study the effects of plate boundary condition, aspect ratio and hole size on the mechanical buckling strength of perforated plates subjected to linearly varying in-plane normal load.

II. Description of the Problem

A. Geometry

The geometry of the perforated rectangular plates and different boundary conditions used in the finite-element analysis are described as follows.

Fig. 1 shows the geometry of perforated rectangular plates with length *l*, width *w* and thickness *t*. The central cutout is a circular hole with diameter *d* (Fig. 1). Table 1 lists the dimensions of perforated rectangular plates.

Notice that all the plates have the same width, w = 20 in. and the same thickness t= 0.1 in.

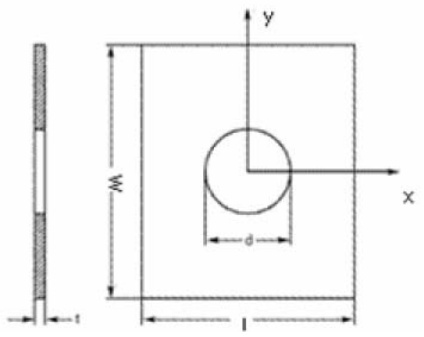

Fig. 1 Rectangular plates with central cutout

A. Boundary Conditions

The four edges of the perforated plates are either simply supported or clamped. The two unloaded edges are either constrained from the transverse in-plane motions (Figs. 2 (a)) which is called fixed case or unconstrained from the transverse in-plane motions (Figs. 2 (b)) that is called free case.

TABLE I
Dimensions Of Perforated Plates

w, in.	20	20	20
t, in	0.1	0.1	0.1
l/w	1	1.5	2.0
d/w	0~0.7	0~0.7	0~0.7

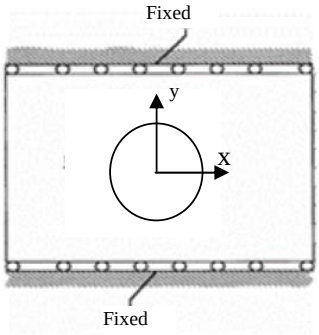

(a) Fixed case-two horizontal edges with no in-plane transverse motion

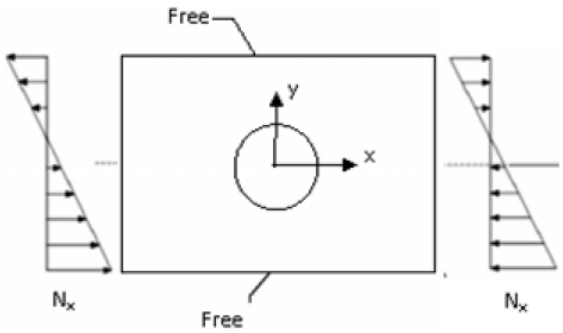

(b) Free case-two horizontal edges with in-plane transverse motion
Fig. 2 Fixed and free boundary condition for two vertical edges (simply supported or clamped)

The four cases of boundary conditions considered in this analysis are as follows:

1. 4S fixed—four edges simply supported; the two side edges can slide freely along the lubricated fixed guides (Fig. 3 (a)).

2. 4S free—four edges simply supported; the two side edges can slide freely along the lubricated guides which can have free in-plane transverse motion (Fig. 3 (b)).

3. 4C fixed—four edges clamped; the two side edges can slide freely along the lubricated fixed clamping guides (Fig. 4 (a)).

4. 4C free—four edges clamped; the two side edges can slide freely along the lubricated clamping guides which can have free in-plane transverse motion (Fig. 4 (b)) [20].

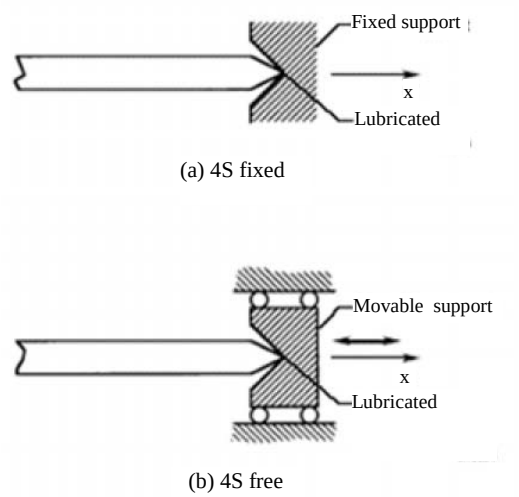

(a) 4S fixed

(b) 4S free

Fig. 3 Two types of boundary conditions for simply-supported horizontal edges

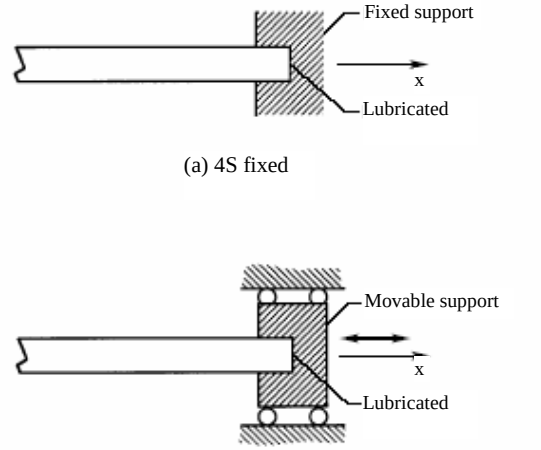

(a) 4S fixed

(b) 4C free

Fig. 4 Two types of boundary conditions for clamped horizontal edges

A linearly varying force is subjected to two opposite edges (x = 0 and x = a) as follows:

$$N_x = -N_0\left(1 - \frac{\alpha}{w}\left(y + \frac{w}{2}\right)\right) \quad (1)$$

where N_0 and α are the intensity of the compressive force per unit length and a numerical factor, respectively [17].

Negative sign in (1) represents compression. By changing α in (1), different particular cases may be obtained. For instance, if α is set to zero, the uniformly distributed compressive force is obtained. By taking α = 1, the compressive force varies linearly from $-N_0$ at y = −w/2 to zero at y = w/2. For α = 2, pure in-plane bending is obtained. The other cases (α = 0.5 and α = 1.5) give a combination of bending and compression. All loading cases are shown in Fig. 5. For simplicity, hereafter the loading cases of α = 0.0, 0.5 and 1.0 are called ‘‘compression”, and a = 1.5 and 2.0 are called ‘‘bending”. The case of α < 0 or α > 2 are not considered because such cases are identical with the cases of 0≤ α ≤ 2 as far as the edge conditions are the same [21,22].

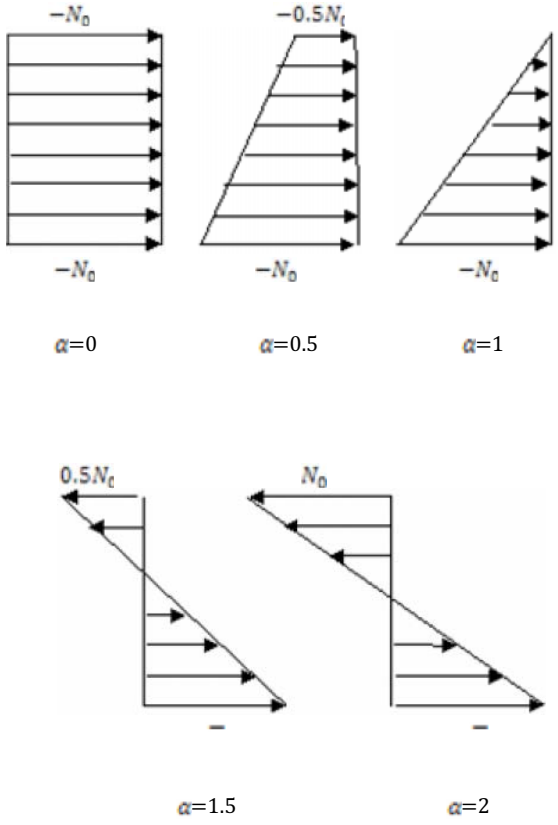

Fig. 5 Example of in-plane loading N_x along the edge

III. Finite Element Analysis Procedure

The commercial multipurpose finite element software program ANSYS (2009) was employed in this research. The general-purpose Elastic Shell63 element is used to model the perforated plate because it shows satisfactory performance in verification work previously described by El-Sawy and Nazmy [14, 15]. The Elastic Shell63 element has four nodes possessing six degrees of freedom per node. An irregular

discretisation in finite element modeling is employed as shown in Fig. 6 in this study. The mesh density of the plate was chosen based on the size of a circular hole. The default shell element size was selected b/50. The shell element size along the hole perimeter was set to the smaller of b/100 or πd/40. The mesh pattern was set-up on the basis of the results achieved in previous numerical studies [15].

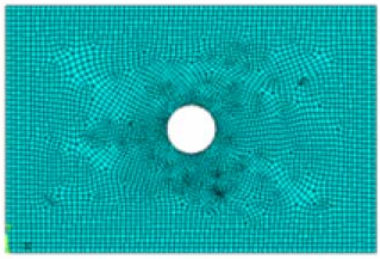

Fig.6 typical mesh of a plate with a circular hole

The material of the plates was assumed to be homogeneous, isotropic and elastic. The material properties for Young's modulus E = 16 × 10^6 lb/in^2 and Poision's ratio υ = 0.31 were selected.

IV. Linear Buckling Analysis

There are two types of buckling analyses: nonlinear buckling analysis and eigenvalue (or linear) buckling analysis. Because the two methods can yield dramatically different results, it is necessary to first understand the differences between them. Nonlinear buckling analysis is usually the more accurate approach and is therefore recommended for design or evaluation of actual structures. This technique employs a nonlinear static analysis with gradually increasing loads to seek the load level at which your structure becomes unstable, as depicted in. Using the nonlinear technique, your model can include features such as initial imperfections, plastic behavior, gaps, and large-deflection response. In addition, using deflection-controlled loading, you can even track the post-buckled performance of your structure (which can be useful in cases where the structure buckles into a stable configuration, such as "snap-through" buckling of a shallow dome).

Eigenvalue buckling analysis predicts the theoretical buckling strength (the bifurcation point) of an ideal linear elastic structure. This method corresponds to the textbook approach to elastic buckling analysis: for instance, an eigenvalue buckling analysis of a column will match the classical Euler solution. However, imperfections and nonlinearities prevent most real-world structures from achieving their theoretical elastic buckling strength. Thus, eigenvalue buckling analysis often yields unconservative results, and should generally not be used in actual day-to-day engineering analyses [23].

The linear buckling analysis will not be suitable if the deformations are not small or if the material shows nonlinear behavior near collapse. In such cases, the nonlinear buckling analysis, which is a combination of both linear and nonlinear buckling analysis, must be performed [17]. In this study, the material behavior is assumed to be linear elastic and deformations compared with the overall dimensions of plate are assumed to be small. Based on the assumptions, the linear buckling analysis is used to determine the critical buckling load of perforated plates.

A general-purpose finite element program, ANSYS, has been utilized in this. The strain used in the formulation includes both the first and second order terms. Therefore, the stiffness matrix generated is composed of the conventional constant small deformation stiffness matrix, K_E, and another matrix, K_σ, which accounts for the effect of the existing stresses, σ , in the plate. The matrix K_σ, called the initial stress stiffness matrix, is found to be proportional to the stress level. Therefore the total stiffness matrix of the plate with stress level σ_0 can be written as

$$K(\sigma_0) = K_E + K_\sigma(\sigma_0) \quad (2)$$

When the stress reaches the level of $\lambda\sigma_0$, the stiffness matrix can be determined as

$$K(\lambda\sigma_0) = K_E + K_\sigma(\lambda\sigma_0) = K_E + \lambda K_\sigma(\sigma_0) \quad (3)$$

Now, the governing equations for the plate behavior can be written as

$$dF = [K_E + \lambda K_\sigma(\sigma_0)]du \quad (4)$$

where du is the incremental displacement vector, and dF is the corresponding incremental force vector. At buckling, the determinant of the stiffness matrix should vanish and the plate exhibits increase in its displacements with no increase in the load. This can be described by

$$|K_E + \lambda K_\sigma(\sigma_0)| = 0 \quad (5)$$

Equation (5) represents an eigenvalue problem, which when solved provides the lowest eigenvalue, λ_1 that corresponds to the critical stress levels $\sigma_{cr} = \lambda_1[\sigma_0]$ at which buckling occurs. In addition, the associated scaled displacement vector $\{u\}$ describes the mode shape at buckling [24].

V. Results and Discussion

For checking the finite-element solution accuracy, the finite-element buckling solution for simply-supported solid plates with no holes and different aspect ratios under uniaxial compression were compared with the corresponding classical buckling solutions [13]. Table 2 shows the results. The classical cases actually correspond to the 4S free cases which are under uniaxial loadings. The 4S fixed cases are slightly under biaxial loadings and therefore, were not used for result comparison.

TABLE II
COMPARISON OF FINITE-ELEMENT AND CLASSICAL BUCKLING SOLUTIONS FOR SIMPLY SUPPORTED RECTANGULAR SOLID PLATES UNDER UNIAXIAL COMPRESSION

l/w	(Nx)cr,lb/in , circular hole model(d=0)	(Nx)cr,lb/in , Timoshenko
1	145.57	145.58
1.5	157.93	157.97
2	145.57	145.58

The comparison of the finite-element and the classical buckling solutions in Table2 shows very close correlation and not only indicates that the adequacy of the finite-element modeling but also provides great confidence in the accuracy of the finite-element buckling solutions for the perforated plates presented in this research.

A. Mechanical Buckling for α = 0 Cases

Figures 7–9, show the compressive buckling loads (α = 0) plotted as functions of hole size *d /w* for the plates with circular holes under 4S-free, 4S-fixed, 4C-free and 4C-fixed boundary conditions. The 4C-free buckling curves almost lie considerably above the other buckling curves for all plate aspect ratios.

For the free and fixed cases, the 4C buckling curves always lie considerably above the 4S buckling curves for all plate aspect ratios. For the 4s fixed cases, by increasing the hole size, the critical buckling load is decreased for all plate aspect ratios. But for the 4C fixed cases, by increasing the hole size, the critical buckling load is increased for all plate aspect ratios. For the other plate-support conditions, it could be decrease or increase and depending on the hole sizes and the plate aspect ratios.

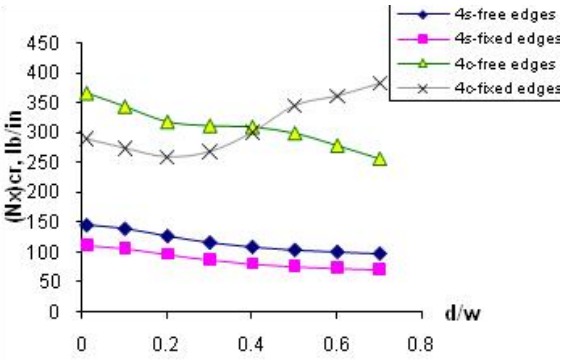

Fig.7 Compressive buckling loads as functions of hole size; circular holes; (l/w=1, α = 0)

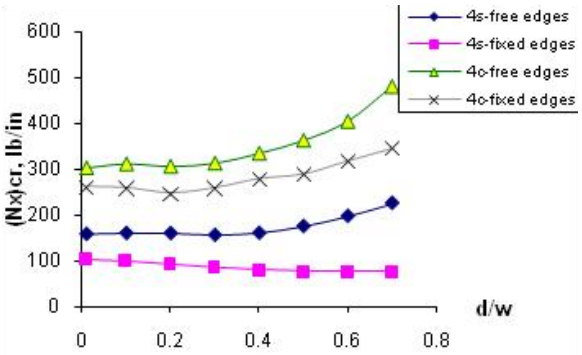

Fig.8 Compressive buckling loads as functions of hole size; circular holes; (l/w=1.5, α =0)

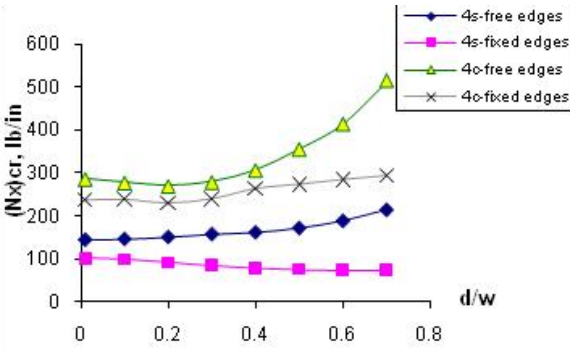

Fig.9 Compressive buckling loads as functions of hole size; circular holes; (l/w=2, α =0)

B. Mechanical Buckling for α = 0.5 and α = 1 Cases

Figures 10–15, show the critical buckling loads for α = 0.5 and α= 1 plotted as function of hole size *d /w* for the plates with circular hole under different boundary conditions. The buckling curves is similar to compressive buckling loads (α = 0).

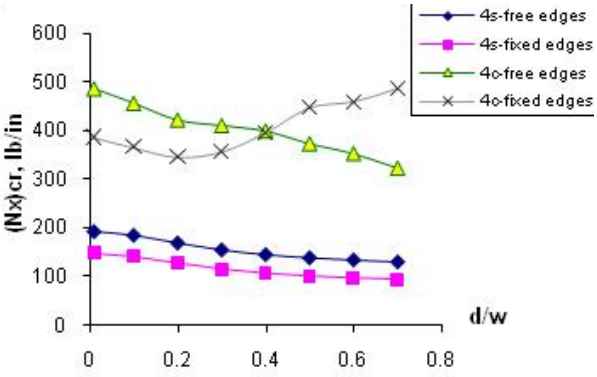

Fig.10 Compressive buckling loads as functions of hole size; circular holes; (l/w=1, α =0.5)

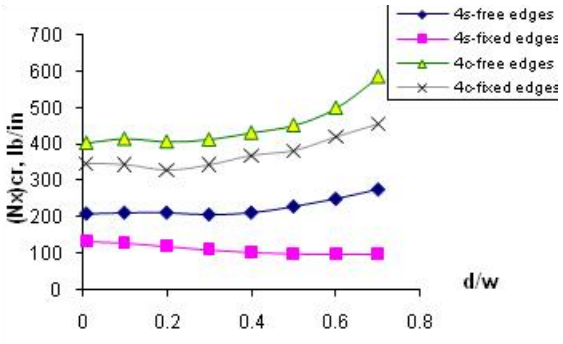

Fig.11 Compressive buckling loads as functions of hole size; circular holes; (l/w=1.5, α =0.5)

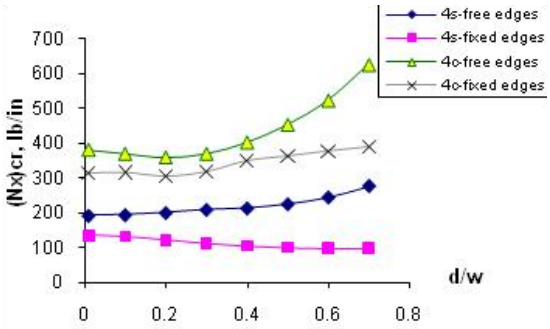

Fig.12 Compressive buckling loads as functions of hole size; circular holes; (l/w=2, α =0.5)

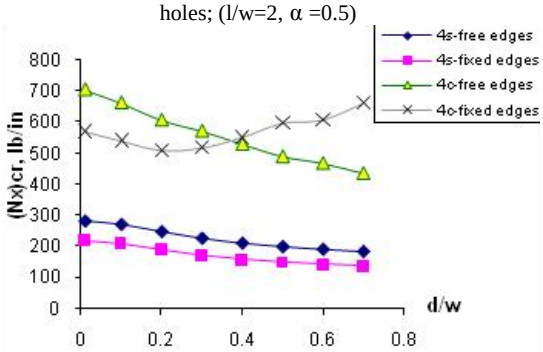

Fig.13 Compressive buckling loads as functions of hole size; circular holes; (l/w=1, α =1)

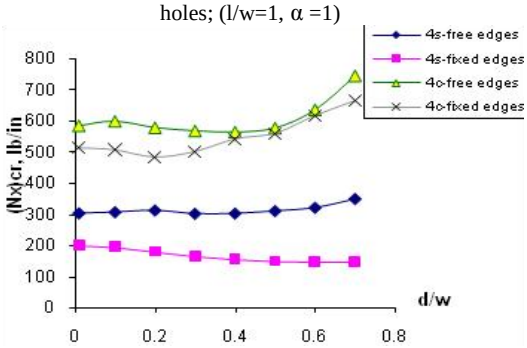

Fig.14. Compressive buckling loads as functions of hole size; circular holes; (l/w=1.5, α =1)

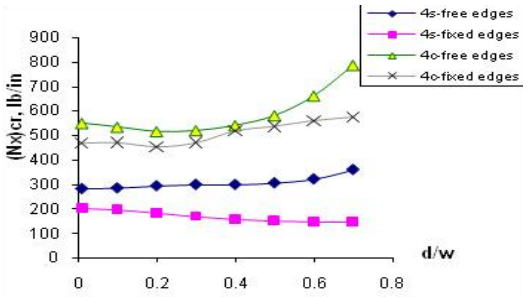

Fig.15. Compressive buckling loads as functions of hole size; circular holes; (l/w=2, α =1)

C. Mechanical Buckling for α = 1.5 Cases

Figures 16–18, show the changes of the critical buckling loads for α = 1.5 with hole size *d* /*w* for the plates with circular hole under different boundary conditions. It can be seen from this figures that for 4S cases, the critical buckling load decrease by increasing the hole size, only when the hole size becomes greater than *d* /*w*=0.5. For 4C cases, the critical buckling load, depending on the hole size and aspect ratio may be decreased or increased.

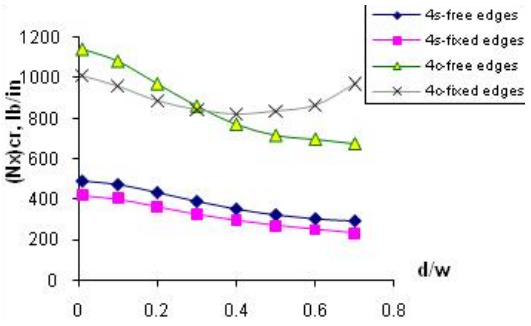

Fig.16 Bending buckling loads as functions of hole size; circular holes; (l/w=1, α =1.5)

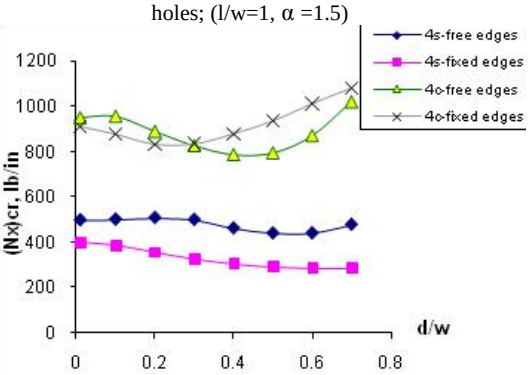

Fig.17. Bending buckling loads as functions of hole size; circular holes; (l/w=1.5, α =1.5)

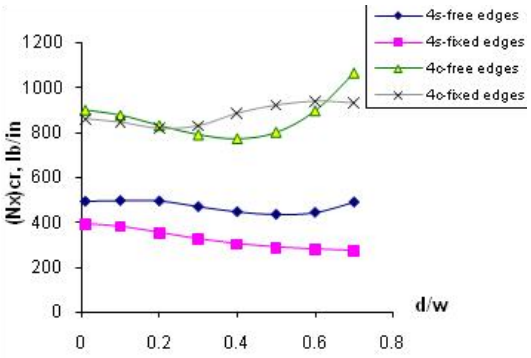

Fig.18 Bending buckling loads as functions of hole size; circular holes; (l/w=2, α =1.5)

D.Mechanical Buckling for α = 2 Cases (Pure Bending)

Figures 19–21, show the pure bending buckling loads (α=2) plotted as function of hole size *d* /*w* for the plates with circular hole under different boundary conditions. The 4C-fixed buckling curves almost lie considerably above the other buckling curves for all plate aspect ratios. The buckling strength for 4S-free condition is almost below the other buckling strength for all plate aspect ratios. For free boundary conditions, the critical buckling loads decrease slightly, as the hole size grows initially, and then increase at larger hole sizes. For 4S-fixed boundary condition, the critical buckling loads always decrease slightly, as the hole size grows. For 4C-fixed boundary condition, the critical buckling loads depending on the aspect ratio may be decreased or increased, as the hole size grows.

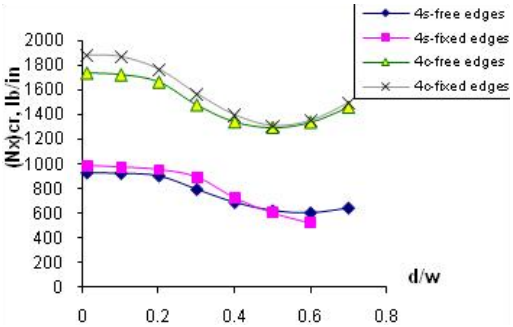

Fig.19 Bending buckling loads as functions of hole size; circular holes; (l/w=2, α 2)

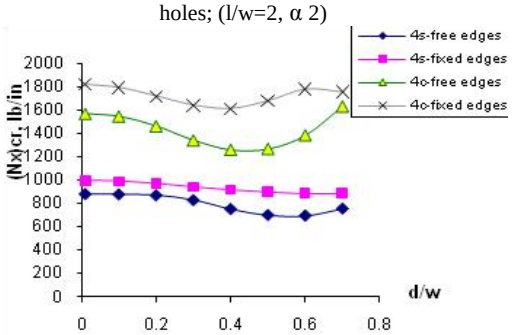

Fig.20 Bending buckling loads as functions of hole size; circular holes; (l/w=1.5, α =2)

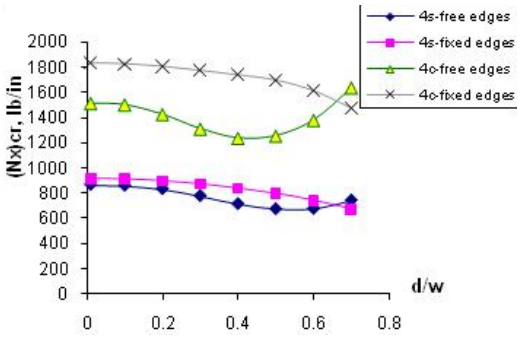

Fig.21 Bending buckling loads as functions of hole size; circular holes; (l/w=2, α =2)

VI. Concluding Remarks

FEM buckling analysis was performed on plates containing centrally located circular hole subjected to linearly varying loading. The effects of plate support conditions, aspect ratio and hole size on the mechanical buckling strength were studied. The key findings of the analysis are as follows:

- Increasing the hole size does not necessarily reduce the mechanical buckling strength of the perforated plates. For certain aspect ratios and support conditions, mechanical buckling strength increase with the increasing hole sizes.
- The clamped boundary conditions increase the mechanical buckling strength of the perforated plates more effectively than the simply-supported boundary conditions.
- For compression loading cases, the free boundary conditions enhance the mechanical buckling strength of the perforated plates more effectively than the fixed boundary conditions. But for bending cases, the fixed boundary conditions increase the mechanical buckling strength of the perforated plates more than the free boundary conditions.

For compression loading cases, by increasing the hole size, the critical buckling loads decrease slightly or increase for some boundary conditions. For bending cases, the critical buckling loads almost decrease as the hole size grows and the presence of the circular hole with d/b = 0.5 and 0.6 causes a reduction on the buckling load up to 30%. These hole sizes is a critical value and must be avoided for bending cases specially in the elastic buckling condition.

References

[1] Levy, Samuel, M. Woolley, And D. Kroll, " Instability of simply supported square plate with reinforced circular hole in edge compression," journal of research, national bureau of standards, vol. 39, research paper no. rp1849, pp. 571–577, dec. 1947.

[2] K. Toyoji, "elastic stability of the square plate with a central circular hole under edge thrust," proc. japan nat. cong. appl. mech, pp. 81–88, 1951.

[3] A. L. Schlack, "Elastic stability of pierced square plates," experimental mechanics, pp. 167–172, june 1964.

[4] A. L. Schlack, "Experimental critical loads for perforated square plates," experimental mechanics, pp. 69–74, feb. 1968.

[5] T.Kawai And H. Ohtsubo, "A method of solution for the complicated buckling problems of elastic plates with combined use of rayleigh-ritz's procedure in the finite element method," affdltr- 68-150, 1968.

[6] Yu, Wei-Wen And Charles S. Davis, "Cold-formed steel members with perforated elements," j. structural division, asce, vol. 99, no. st10, pp. 2061–2077, oct. 1973.

[7] D. Ritchie, And J. Rhodes, "Buckling and post-buckling behaviour of plates with holes," aeronautical quarterly, vol. 26, pp. 281–296, nov. 1975.

[8] M. Nemeth, " Buckling behavior of orthotropic composite plates with centrally located cutouts," ph. d. dissertation, virginia polytechnic institute and state university, may 1983.

[9] M. Nemeth, "A buckling analysis for rectangular orthotropic plates with centrally located cutouts," nasa tm-86263, dec. 1984.

[10] M. Nemeth, M. Stein, And E. R. Johnson, "An approximate buckling analysis for rectangular orthotropic plates with centrally located cutouts," nasa tp-2528, feb. 1986.

[11] M. Nemeth, "Buckling behavior of compression-loaded symmetrically laminated angle-ply plates with holes," aiaa journal, vol. 26, no. 3, pp. 330–336, mar. 1988.

[12] Y. J. Lee, H. J. Lin, And C. C. Lin, "A study on the buckling behavior of an orthotropic square plate with a central circular hole," composite structures, vol. 13, no. 3, pp.173–188, 1989.

[13] S. Timoshenko And J. M. Gere, "*Theory Of Elastic Stability*," 2nd ed., mcgraw-hill book company, new york, 1961.

[14] K.M. El-Sawy, A.S. Nazmy, M.I. Martini, "Elasto-plastic buckling of perforated plates under uniaxial compression," thin-walled structures 42, 1083–1101, 2004.

[15] K.M. El-Sawy, A.S. Nazmy, "Effect of aspect ratio on the elastic buckling of uniaxially loaded plates with eccentric holes," thin-walled structures; 39(12):983–98, 2001.

[16] C.J. Brown, A.L. Yettram, " Factors influencing the elastic stability of orthotropic plates containing a rectangular cut-out," journal of strain analysis for engineering design; 35(6):445–58, 2000.

[17] A. Komur, M. Sonmez, " Elastic buckling of rectangular plates under linearly varying in-plane normal load with a circular cutout," mechanics research communications; 35(6):361–71, 2008.

[18] E. Maiorana, C. Pellegrino, C. Modena, "Elastic stability of plates with circular and rectangular holes subjected to axial compression and bending moment," thin-walled structures; 47(3):241–55, 2009.

[19] C. Moen, B. Schafer, "Impact of holes on the elastic buckling of cold-formed steel columns with applications to the direct strength method," in: eighteenth international specialty conference on cold-formed steel structures. orlando, fl; p.269–83, 2006.

[20] L. William, "Mechanical- and thermal-buckling behavior of rectangular plates with different central cutouts," nasa dryden flight research center, 1998.

[21] J.H. Kang, A.W. Leissa, "Exact solutions for the buckling rectangular plates having linearly varying in-plane loading on two opposite simply supported edges," international journal of solids and structures 42, 4220–4238, 2005.

[22] A.W. Leissa, J.H. Kang, "Exact solutions for vibration and buckling of an ss-c-ss-c rectangular plate loaded by linearly varying in-plane stresses," international journal of mechanical sciences 44, 1925–1945, 2002.

[23] ANSYS, 2009. user manual, version 11.0, ansys, inc.

[24] K.M. El-Sawy, A.S. Nazmy, "Effect of aspect ratio on the elastic buckling of uniaxially loaded plates with eccentric holes," thin-walled structures 39, 983–998, 2001.